nature nanotechnology

LETTERS

PUBLISHED ONLINE: 19 MAY 2013 | DOI: 10.1038/NNANO.2013.84

A transparent electrode based on a metal nanotrough network

Hui Wu[1,2†], Desheng Kong[1†], Zhichao Ruan[3], Po-Chun Hsu[1], Shuang Wang[3], Zongfu Yu[3], Thomas J. Carney[1], Liangbing Hu[1], Shanhui Fan[3] and Yi Cui[1,4*]

Transparent conducting electrodes are essential components for numerous flexible optoelectronic devices, including touch screens and interactive electronics[1–4]. Thin films of indium tin oxide—the prototypical transparent electrode material—demonstrate excellent electronic performances, but film brittleness, low infrared transmittance and low abundance limit suitability for certain industrial applications[1,4,5]. Alternatives to indium tin oxide have recently been reported and include conducting polymers[6], carbon nanotubes[7–9] and graphene[10–12]. However, although flexibility is greatly improved, the optoelectronic performance of these carbon-based materials is limited by low conductivity[8,13]. Other examples include metal nanowire-based electrodes[14–22], which can achieve sheet resistances of less than $10\Omega\square^{-1}$ at 90% transmission because of the high conductivity of the metals. To achieve these performances, however, metal nanowires must be defect-free, have conductivities close to their values in bulk, be as long as possible to minimize the number of wire-to-wire junctions, and exhibit small junction resistance. Here, we present a facile fabrication process that allows us to satisfy all these requirements and fabricate a new kind of transparent conducting electrode that exhibits both superior optoelectronic performances (sheet resistance of $\sim 2\Omega\square^{-1}$ at 90% transmission) and remarkable mechanical flexibility under both stretching and bending stresses. The electrode is composed of a free-standing metallic nanotrough network and is produced with a process involving electrospinning and metal deposition. We demonstrate the practical suitability of our transparent conducting electrode by fabricating a flexible touch-screen device and a transparent conducting tape.

The process for fabricating our nanotrough network is based on templating ultralong polymer nanofibres (Fig. 1a). In the first step, continuous polymer nanofibre webs are prepared by means of electrospinning[23], a low-cost and scalable approach for forming long polymer fibres assembled in random networks or oriented arrays controlled by the geometry of the fibre collector (Supplementary Fig. S1). Note that the electrospun fibres can bridge an extremely long distance (across a gap of more 6 inches, as shown in Supplementary Fig. S2). In the second step, the free-standing polymer nanofibre networks are coated with a thin layer of material using standard thin-film deposition techniques, such as thermal evaporation, electron-beam evaporation or magnetron sputtering[24], allowing a rich variety of functional materials to be prepared while retaining a bulk-like electrical conductivity. Owing to the directionality of these deposition processes[24], the polymer fibres are preferentially coated on one side, thus forming nanotroughs with a concave cross-section (Fig. 1c, Supplementary Fig. S3). The coated polymer fibres are mechanically flexible and robust, and can be transferred easily onto various substrates to interface with macroscopic-scale systems. In the third step, after transferring the fibre, the polymer templates are removed by submerging the entire electrode in water or other organic solvents. Using this method, we have fabricated continuous nanotrough networks from a wide variety of functional materials, including silicon, indium tin oxide (ITO) (Supplementary Fig. S4) and metals such as gold (Fig. 1b), silver, copper, platinum, aluminium, chromium, nickel and their alloys (Supplementary Fig. S5).

The microstructure of the nanotroughs was characterized by scanning electron microscopy (SEM). Figure 1b shows a typical example of a nanotrough network, in this case a uniform network of intertwined gold nanotroughs with widths of ~400 nm and lengths greater than 1 mm. It is important to note that individual nanotroughs are naturally interconnected at their junctions during metal deposition (Fig. 1b). A side-view SEM image of the synthesized nanotroughs (Fig. 1c) confirms that polymer fibre templates have been fully removed, leaving solid ribbons with concave cross-sections. The thickness of each trough is ~80 nm, and can be varied easily by changing the metal deposition time. The average width of each trough is 406 nm (Supplementary Fig. S6) and can be adjusted by controlling the diameter of the polymer fibre template by means of electrospinning. Figure 1d shows examples of gold nanotroughs successfully attached to different surfaces, including a glass slide, polyethylene terephthalate (PET) plastic, paper, a textile and a curved glass flask, all without any surface treatment, and making all the surfaces highly conducting (Fig. 1d, Supplementary Fig. S9). The nanotroughs are firmly attached to the substrates (Supplementary Fig. S7) and cannot be peeled off with scotch tape (Supplementary Movie S1).

Metal films with thicknesses greater than 80 nm usually have low transmittance[25], but our metal nanotroughs are highly transparent (Supplementary Fig. S10). Figure 2a plots the transmittance of the metal nanotrough electrodes on glass substrates with various sheet resistances R_s. The R_s values of copper, gold and silver nanotroughs with ~90% optical transmittance are ~2, 8 and $10\Omega\square^{-1}$, respectively. Copper nanotrough networks demonstrated the best performance—$2\Omega\square^{-1}$ at $T = 90\%$, $10\Omega\square^{-1}$ at $T = 95\%$ and $17\Omega\square^{-1}$ at $T = 97\%$—a performance that is comparable to state-of-the-art device-grade ITO[20] and superior to other transparent conducting electrodes such as those based on graphene, carbon-nanotube films, solution-processed silver or copper nanowires, metal grids, thin metal films and conducting polymers (Fig. 2a)[7,8,12,14,16,17,20,25–27].

[1]Department of Materials Science and Engineering, Stanford University, California 94305, USA, [2]State Key Lab of New Ceramics and Fine Processing, School of Materials Science and Engineering, Tsinghua University, Beijing 100084, China, [3]Department of Electrical Engineering, Stanford University, California 94305, USA, [4]Stanford Institute for Materials and Energy Sciences, SLAC National Accelerator Laboratory, 2575 Sand Hill Road, Menlo Park, California 94025, USA, †These authors contributed equally to this work. *e-mail: yicui@stanford.edu

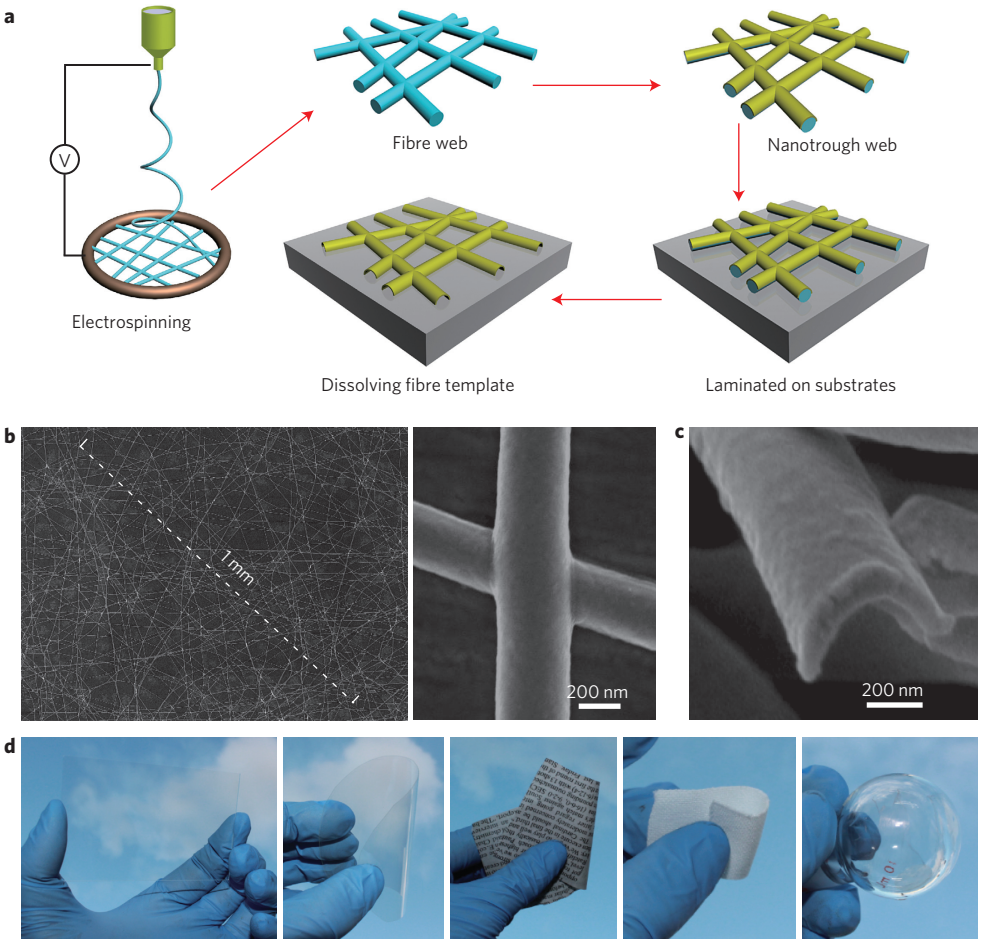

Figure 1 | Fabrication and transfer process for nanotroughs. a, Schematic of the polymer-nanofibre templating process for fabricating nanotroughs. Polymer nanofibre templates were first made by electrospinning, then coated with selected materials using standard thin-film deposition techniques. The coated fibres were transferred onto a solid substrate. The substrate was subsequently dipped in water or an organic solvent to dissolve away the polymer-fibre template. **b**, Top-view SEM images of gold nanotrough networks (left) and a junction between two nanotroughs (right). **c**, SEM image of the cross-section of a single gold nanotrough, revealing its concave shape. **d**, Gold nanotrough networks can be transferred easily onto various substrates, including a glass slide, PET plastic, paper, textile and a curved glass flask (left to right).

The remarkable performance of nanotrough electrodes can be attributed to several main factors. First, the metal nanotroughs are produced using a standard thin-film deposition process, which yields high-quality metals. For example, a single gold nanotrough has an electric conductivity of $\sim 2.2 \times 10^5$ S cm^{-1} (measured by a four-point probe), which is comparable to its polycrystalline bulk value (4.1×10^5 S cm^{-1}) (Fig. 2b, Supplementary Figs S12 and S13). It is important to note that nanostructured metals usually have significantly lower conductivity compared to their bulk counterpart, possibly due to impurities incorporated during synthesis, reduced crystal quality, contaminants or surfactants on the surface, and electron scattering. For example, the conductivity of a single-crystalline silver nanowire is approximately ten times lower than that of the bulk crystal[28]. In contrast, our nanotroughs exhibit an electrical conductivity that is approximately half that of the bulk, possibly a result of the evaporation process, which produces clean and high-quality metals.

Second, the nanotroughs form a highly uniform, interconnected network. The properties of these nanotrough electrodes are well described by percolation theory (Supplementary Fig. S11)[29]. These nanotrough networks are required to have exceptional percolation parameters to achieve high-performance transparent conducting electrodes (Supplementary Table S1). It has been shown that percolation parameters largely depend on the uniformity of the network[22]. The improvement observed here can therefore be ascribed to the spatially uniform network that is a consequence of the evenly distributed polymer nanofibre template achieved by the electrospinning process. The interconnected structure of the nanotrough network (Fig. 1b) also avoids the creation of a large junction resistance, a common bottleneck in metal nanowire networks[15].

Third, the concave shape of the nanotroughs reduces the electromagnetic cross-section, which allows more visible light to pass through in comparison to flat nanostripes (Supplementary Fig. S15).

The metal nanotrough networks demonstrate flat transmittance spectra from 300 nm to 2,000 nm (Fig. 2c, Supplementary Fig. S16). Wideband flat spectra are highly desirable for many optoelectronic devices as they simplify the optics by removing additional chromatic correction components, enable applications in near-infrared sensors and detectors, and may enhance solar cell efficiency by using the near-infrared solar spectrum (where conventional ITO conductors become almost opaque[3]).

Chemical stability is another important concern for transparent conducting electrodes. Supplementary Fig. S17 shows the change in resistance in various metal nanotrough networks upon exposure to high temperatures and humidity. The chemical stability can be improved significantly with surface passivation, as demonstrated

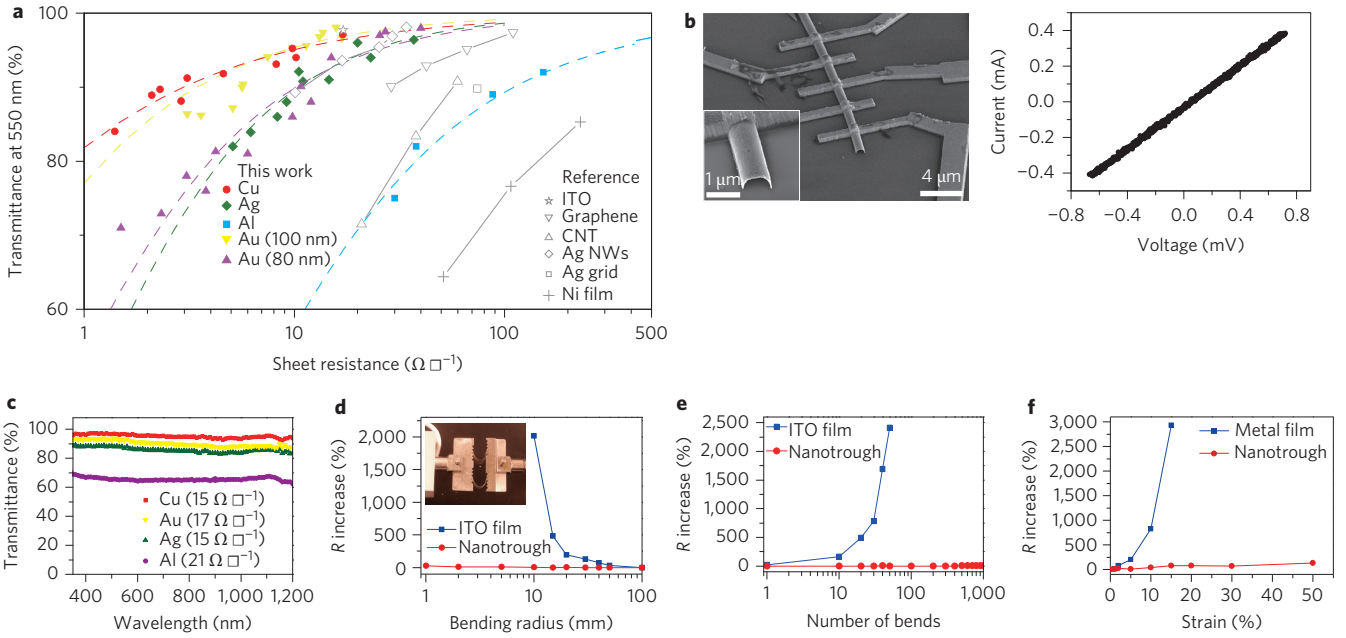

Figure 2 | Metal nanotrough networks as transparent, flexible electrodes. a, Sheet resistance versus optical transmission (at 550 nm) for copper, gold, silver and aluminium nanotrough networks, described by percolation theory (details of fitting are presented in Supplementary Fig. S11 and Table S1). The performances of device-grade ITO (ref. 20), carbon nanotubes (CNTs)[8], graphene[12], silver nanowires (NWs)[20], silver grid[27] and nickel thin films[25] are shown for comparison. Note that the transmittance mentioned here does not include the transmittance of the substrate. **b**, Four-terminal electrical conductivity measurement for a single gold nanotrough. Left: tilted SEM images of the single nanotrough device; right: *I*–*V* curve for the single nanotrough device. Additional electrical conductivity measurements on single nanotroughs are provided in Supplementary Figs S12–S14. **c**, UV–vis spectra of metal nanotrough networks on glass substrates, showing a very flat spectrum for the entire wavelength range. **d**, R_s versus bending radius for bendable transparent electrodes consisting of gold nanotrough networks or ITO films on 178-μm-thick PET substrates. **e**, Variations in resistance of a gold nanotrough electrode and an ITO electrode on PET film as a function of the number of cycles of repeated bending to a radius of 10 mm. **f**, R_s versus uniaxial strain for a stretchable transparent electrode consisting of gold nanotrough networks on 0.5-mm-thick PDMS substrate. The rapid degradation of a gold thin film with a thickness similar to the nanotroughs (80 nm) is shown.

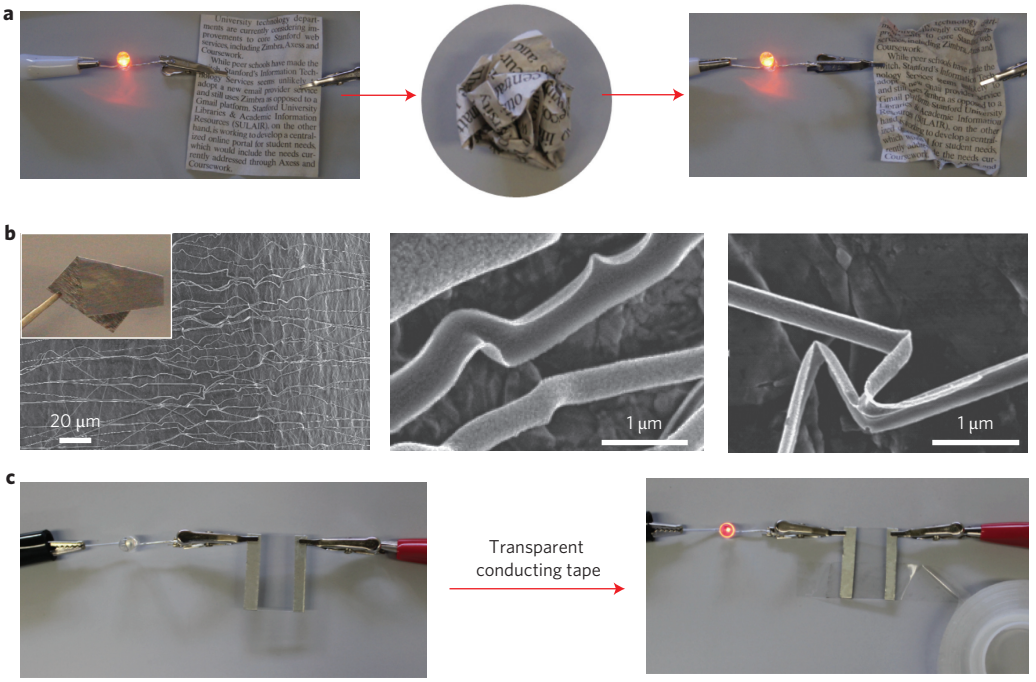

Figure 3 | Foldable, transparent, metal-nanotrough electrodes. a, Photographs of 'conducting paper', fabricated by transferring gold nanotrough networks onto paper. After crushing and unfolding, the paper remained conducting (resistance increasing from 73 Ω to 131 Ω). **b**, SEM images of gold nanotroughs on aluminium foil after folding. **c**, By transferring gold nanotroughs onto the sticky side of commercial transparent tape, the tape became conductive (with a resistance of 22 Ω between the two electrodes) while retaining its flexibility and transparency. (See Supplementary Movie S2 of the operation of this transparent conducting tape.)

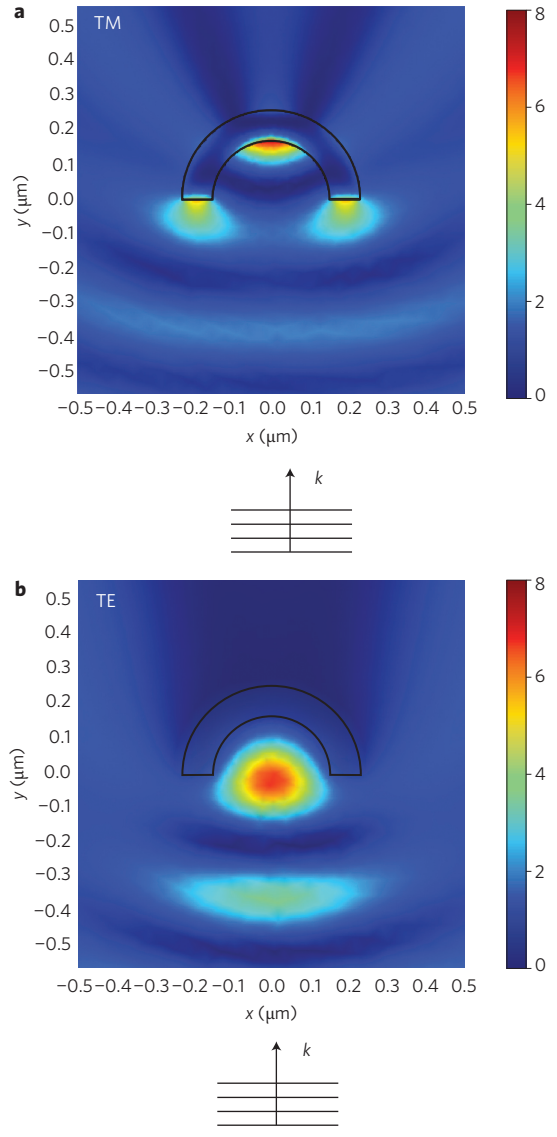

Figure 4 | Optical simulation of a single metal nanotrough. a,**b**, Intensity distribution of TM (**a**) and TE (**b**) fields in the vicinity of a gold nanotrough, at a wavelength of 540 nm, where a plane wave with unitary amplitude is incident on the nanotrough from bottom to top. The diameter and thickness of the nanotrough are 460 nm and 80 nm, respectively. Simulation is performed by numerically solving Maxwell's equations using a finite-element method (CMSOL) in two-dimensional space.

in our previous study on copper nanofibres[30]. Passivation of the nanotroughs is beyond the scope of the current study and will be a valid future research topic.

Our metal nanotrough networks are bendable, stretchable and foldable. To examine their mechanical durability, we transferred the networks onto a 178-μm-thick PET substrate and either bent the film down to a radius of 2 mm (Fig. 2d) or repetitively bent the film to 20 mm, 2,000 times (Fig. 2e). On examining the transparent electrode after both bending regimes, we could find no obvious degradation in electrical conductivity. In contrast, severe degradation in conductivity is observed in ITO films after bending to $<$50 mm, or bending to 20 mm more than 20 times (Fig. 2d,e). The stretchability of the transparent electrodes was examined by transferring the nanotrough networks onto a substrate of poly(dimethylsiloxane) (PDMS) without surface activation. The sheet resistance increased by ~40% after being stretched uniaxially to 50% strain, which is comparable to the performance of carbon-nanotube-based transparent elastic conductors[2] and in great contrast to the dramatic increase in resistance observed in metal films of similar thickness (Fig. 2f).

We also transferred nanotrough networks onto paper to test their mechanical properties under extreme conditions. After crushing and then unfolding the electrode on paper, the electrode remained conductive, with only a limited change in the resistance (Fig. 3a, Supplementary Fig. S18). The mechanistic explanation is that the nanotroughs remain continuous during folding, undergoing nanoscale deformation to relax the applied stress (Fig. 3b). Moreover, SEM images show that a free-standing metal nanotrough network can be folded without fracturing (Supplementary Fig. S19). These durable nanotrough networks can also be transferred onto commercial cellulose tape to produce transparent conducting tape (Fig. 3c, Supplementary Movie S2). This transparent conducting tape can stick easily onto a material surface, making the surface conductive without any surface treatment. This new technique may enable easy integration of optoelectronic devices and possibly expand the areas of application of transparent conducting electrodes.

Because of the many advantages of metal nanotrough electrodes, including facile fabrication, ease of transfer, high transparency and superior flexibility, these electrodes are readily applicable in practical optoelectronic devices. Indeed, we have demonstrated a high-performance nanotrough electrode incorporated into a resistive touch-screen device (Supplementary Fig. S20). The operation of this device is demonstrated in Supplementary Movie S3.

Finally, the unique concave shape and nanoscale dimensions of our continuous metal nanotroughs also lead to interesting optical properties. To understand the interaction between an incident light field and the nanotrough, we numerically solved Maxwell's equations and obtained the near-field distribution of light intensity around the nanotrough. Our simulation predicts a localized 'light-focusing' phenomenon associated with this structure, which effectively concentrates light in the vicinity of the metal nanotroughs (Fig. 4). For transverse magnetic (TM) polarization (Fig. 4a), the field intensity is enhanced almost seven times around the inner boundary of the ribbon due to well-known surface plasmonic effects. Interestingly, for transverse electrical (TE) polarization, even without the surface plasmonic effect the nanotroughs still provide a significant light concentration effect, with the field intensity enhanced by a factor of about 6.5 at the centre (Fig. 4b). This is due to the unique cross-section of the ribbon, which mimics the action of a macroscopic trough reflector to maximize the field intensity at the centre. The novel localized light (or energy) concentration effects are expected to be useful for many optoelectronic applications, including solar cells, solar fuels, photo-assisted localized chemical reactions and optical sensors.

In summary, we have shown that metal nanotrough transparent conducting electrodes exhibit both excellent optoelectronic performance (to compete with device-grade ITO) and remarkable mechanical properties (to tolerate large bending and stretching stresses). Their synthesis is facile and amenable to scale up based on standard electrospinning and metal deposition techniques. Such metal nanotrough electrodes could replace ITO, which is widely used in solar cells, touch sensors and flat panel displays, and could find use in emerging application areas such as flexible electronics and skin-like sensors[2].

Methods

Nanotrough fabrication. The polymer nanofibre template was produced using electrospinning, a well-known technique for making continuous ultralong nanofibres at low cost and in large quantity. Water-soluble polymers including polyvinyl alcohol (PVA, Sigma-Aldrich) and polyvinylpyrrolidone (PVP, Sigma-Aldrich) were selected as the raw materials to produce naturally degradable polymer templates. The precursor solution was made by adding polymer powder (10 wt% PVA or 14 wt% PVP) to deionized water then stirring at 80 °C for 10 h.

A voltage of 15 kV was applied to the solution using a high-voltage source (Gamma High Voltage Research, model ES30P-5W) to spin fibres out of a needle. The free-standing fibres gradually formed a network, which was collected in a copper frame. The density of nanofibres could be controlled by altering the electrospinning time. Metal nanotroughs were prepared at a base pressure of 1×10^{-6} torr by thermal evaporation (Mbraun glovebox integrated evaporator system) of chromium, gold, copper, silver and aluminium, and electron-beam evaporation (Temescal electron-beam evaporator) of platinum and nickel. For the metal nanotrough networks used as transparent electrodes, a constant thickness of 100 nm was deposited for all metals, unless otherwise specified. The sample temperature was kept below 60 °C during evaporation. Silicon and ITO nanotroughs were generated based on a.c. magnetosputtering (AJA ORION sputtering system) with a low power of 125 W and a pressure of 5 mtorr. Note that the quality of the nanotroughs was affected by the choice of polymer templates (Supplementary Fig. S8). Accordingly, PVP nanofibre templates were selected for the nanotroughs of gold, platinum, silicon and ITO, whereas PVA nanofibre templates were used for copper, silver and aluminium.

Optical and electrical characterization. The sheet resistances of the films were measured using a digital multimeter (Keithley 2100) with a four-point probe configuration to eliminate contact resistance. The conductivity of the nanotroughs was determined using a single nanotrough device. The conductive networks were sonicated in ethanol to form a suspension containing individual nanotroughs. The nanotroughs were dropcast onto an oxidized silicon substrate and patterned into devices by means of standard electron-beam photolithography and thermal evaporation of chromium/gold (10 nm/190 nm) contacts. The nanotrough device was then measured using an Agilent B1500A semiconductor device analyser. The transmittance measurement used a quartz tungsten halogen lamp as the light source, coupled with a monochromator (Newport 70528) to control the wavelength. An iris and a convex lens were used to focus the beam size to ~1 mm × 2 mm, and a beamsplitter split the light beam into an integrating sphere (Newport, for transmittance measurement) and a photodiode (Newport, 818-UV-L). The photodiode was connected to an electrometer (Keithley 6517A) for light intensity calibration. The samples were placed in front of the integrating sphere, so specular light, diffuse light and haze were all included. An identical glass slide was used for reference. A source-measure unit (Keithley 236) was used to measure the photocurrent from the integrating sphere, and the transmittance was thus calculated based on the reference plain glass slide. Accordingly, the measured transmittance did not include the transmittance of the glass substrates.

Touch-screen device fabrication. The four-wire analogue-resistive touch-screen device was rebuilt from a commercial product from TVI Electronics. The 2.8-inch device consisted of an ITO electrode on a PET film and a piece of ITO glass, which were separated by square arrays of polymer spacer dots. In the rebuilt device, the ITO/PET film was replaced with a gold nanotrough network on 178-μm-thick PET. To prepare the gold nanotrough transparent conducting electrode component, the gold nanotrough network was transferred onto the PET substrate, and then patterned with a 400-nm-thick copper circuit with the aid of a plastic hard mask. The copper circuit allowed the gold nanotrough electrode to connect with a commercial controller (also from TVI Electronics), which interfaced with the computer. The sandwich-structure device was finally sealed with double-sided tape. Testing software was also provided by the vendor.

Received 26 July 2012; accepted 11 April 2013;
published online 19 May 2013

References

1. Fortunato, E., Ginley, D., Hosono, H. & Paine, D. C. Transparent conducting oxides for photovoltaics. *Mater. Res. Soc. Bull.* **32,** 242–247 (2007).
2. Lipomi, D. J. *et al.* Skin-like pressure and strain sensors based on transparent elastic films of carbon nanotubes. *Nature Nanotech.* **6,** 788–792 (2011).
3. Peng, H. L. *et al.* Topological insulator nanostructures for near-infrared transparent flexible electrodes. *Nature Chem.* **4,** 281–286 (2012).
4. Kumar, A. & Zhou, C. W. The race to replace tin-doped indium oxide: which material will win? *ACS Nano* **4,** 11–14 (2010).
5. Tahar, R. B. H., Ban, T., Ohya, Y. & Takahashi, Y. Tin doped indium oxide thin films: electrical properties. *J. Appl. Phys.* **83,** 2631–2645 (1998).
6. Kirchmeyer, S. & Reuter, K. Scientific importance, properties and growing applications of poly(3,4-ethylenedioxythiophene). *J. Mater. Chem.* **15,** 2077–2088 (2005).
7. Zhang, M. *et al.* Strong, transparent, multifunctional, carbon nanotube sheets. *Science* **309,** 1215–1219 (2005).
8. Hecht, D. S., Hu, L. B. & Irvin, G. Emerging transparent electrodes based on thin films of carbon nanotubes, graphene, and metallic nanostructures. *Adv. Mater.* **23,** 1482–1513 (2011).
9. Niu, C. M. Carbon nanotube transparent conducting films. *Mater. Res. Soc. Bull.* **36,** 766–773 (2011).
10. Kim, K. S. *et al.* Large-scale pattern growth of graphene films for stretchable transparent electrodes. *Nature* **457,** 706–710 (2009).
11. Bonaccorso, F., Sun, Z., Hasan, T. & Ferrari, A. C. Graphene photonics and optoelectronics. *Nature Photon.* **4,** 611–622 (2010).
12. Bae, S. *et al.* Roll-to-roll production of 30-inch graphene films for transparent electrodes. *Nature Nanotech.* **5,** 574–578 (2010).
13. Hecht, D. S. & Kaner, R. B. Solution-processed transparent electrodes. *Mater. Res. Soc. Bull.* **36,** 749–755 (2011).
14. De, S. *et al.* Silver nanowire networks as flexible, transparent, conducting films: extremely high DC to optical conductivity ratios. *ACS Nano* **3,** 1767–1774 (2009).
15. Garnett, E. C. *et al.* Self-limited plasmonic welding of silver nanowire junctions. *Nature Mater.* **11,** 241–249 (2012).
16. Hu, L. B., Wu, H. & Cui, Y. Metal nanogrids, nanowires, and nanofibres for transparent electrodes. *Mater. Res. Soc. Bull.* **36,** 760–765 (2011).
17. Wu, H. *et al.* Electrospun metal nanofibre webs as high-performance transparent electrode. *Nano Lett.* **10,** 4242–4248 (2010).
18. Kang, M. G., Kim, M. S., Kim, J. S. & Guo, L. J. Organic solar cells using nanoimprinted transparent metal electrodes. *Adv. Mater.* **20,** 4408–4413 (2008).
19. Van de Groep, J. V., Spinelli, P. & Polman, A. Transparent conducting silver nanowire networks. *Nano Lett.* **12,** 3138–3144 (2012).
20. Leem, D. S. *et al.* Efficient organic solar cells with solution-processed silver nanowire electrodes. *Adv. Mater.* **23,** 4371–4375 (2011).
21. Lyons, P. E. *et al.* High-performance transparent conductors from networks of gold nanowires. *J. Phys. Chem. Lett.* **2,** 3058–3062 (2011).
22. Scardaci, V., Coull, R., Lyons, P. E. Rickard, D. & Coleman, J. N. Spray deposition of highly transparent, low-resistance networks of silver nanowires over large areas. *Small* **7,** 2621–2628 (2011).
23. Li, D. & Xia, Y. N. Electrospinning of nanofibres: Reinventing the wheel? *Adv. Mater.* **16,** 1151–1170 (2004).
24. Kelly, P. J. & Arnell, R. D. Magnetron sputtering: a review of recent developments and applications. *Vacuum* **56,** 159–172 (2000).
25. Ghosh, D. S. Martinez, L., Giurgola, S., Vergani, P. & Pruneri, V. Widely transparent electrodes based on ultrathin metals. *Opt. Lett.* **34,** 325–327 (2009).
26. Lipomi, D. J. *et al.* Electronic properties of transparent conductive films of PEDOT:PSS on stretchable substrates. *Chem. Mater.* **24,** 373–382 (2012).
27. Lee, J-Y., Connor, S. T., Cui, Y. & Peumans, P. Solution-processed metal nanowire mesh transparent electrodes. *Nano Lett.* **8,** 689–692 (2008).
28. Sun, Y. G., Gates, B., Mayers, B. & Xia, Y. N. Crystalline silver nanowires by soft solution processing. *Nano Lett.* **2,** 165–168 (2002).
29. De, S. & Coleman, J. N. The effects of percolation in nanostructured transparent conductors. *Mater. Res. Soc. Bull.* **36,** 774–781 (2011).
30. Hsu, P. C. *et al.* Passivation coating on electrospun copper nanofibres for stable transparent electrodes. *ACS Nano* **6,** 5150–5156 (2012).

Acknowledgements

This material is based upon work supported as part of the Center on Nanostructuring for Efficient Energy Conversion (CNEEC) at Stanford University, an Energy Frontier Research Center funded by the US Department of Energy, Office of Science, Office of Basic Energy Sciences under Award Number DE-SC0001060, and the National Basic Research of China (grant no. 2013CB632702).

Author contributions

H.W. and Y.C. conceived the idea. H.W. and D.K. performed materials fabrication and tests. Z.C.R., Z.F.Y. and S.H.F. designed and carried out the optical simulations. H.W. and D.K. co-wrote the paper. All authors discussed the results and commented on the manuscript.

Additional information

Supplementary information is available in the online version of the paper. Reprints and permissions information is available online at www.nature.com/reprints. Correspondence and requests for materials should be addressed to Y.C.

Competing financial interests

The authors declare no competing financial interests.